Multifractality in Humanitarian Applications: A Case Study of Internally Displaced Persons/Refugee Camps

Małgorzata Jenerowicz, Anna Wawrzaszek, Wojciech Drzewiecki, Michał Krupiński, and Sebastian Aleksandrowicz

***Abstract*—The coordination of humanitarian relief is always difficult due to a lack of data required for management and planning. Remote sensing imagery can be an important source of information about the in-situ situation, notably, no-access areas. Scenarios include situation awareness after natural disasters or military conflicts, damage assessment, or monitoring camp structure, either as a one-off exercise or on an ongoing basis. In this article, we propose a multifractal approach to automating information extraction about internally displaced persons/refugee camps and discuss its potential and limitations. Our case study uses multifractal features to determine the extent of camps in Kenya and Sudan. The results show that the method can be usefully applied to camp growing analysis and help to make a rough, but rapid estimation of their extent. Our multifractal method appears to be a reasonable step forward on the road between manual mapping and (not yet developed) fully automated, highly accurate processing.**

***Index Terms*—Feature extraction, multifractal, refugee/internally displaced persons (IDPs) monitoring, settlement mapping, very high resolution (VHR) satellite images.**

I. Introduction

LONG-TERM humanitarian relief requires reliable and comprehensive information that is constantly delivered during a crisis. However, the support that decision-makers need, notably through repeated surveys of the situation on the ground, is often unfeasible, especially over large areas. This situation has led to the use of remote sensing data in the humanitarian domain. Remote sensing is already being used to monitor and guide humanitarian responses to conflicts, human rights violations, and man-made or natural disasters [1]–[4].

Satellite data are especially valuable in difficult-to-reach or dangerous zones where *in-situ* measurements and observations are sparse or nonexistent [5], [6]. In particular, very high resolution (VHR) optical satellite data have been shown to be useful in monitoring internally displaced persons (IDPs)/refugee camps as it can provide an overview of the affected areas with spatial resolution of up to 0.3 m within a matter of days (depending on certain factors, including a cloud cover). According to the United Nations High Commissioner of Refugees (UNHCR), approximately 70.8 million people worldwide were forced to leave their homes by the end of 2018 [7]. At this time, the total number of people targeted by UNHCR reached 74.8 million. This included people who had been forcibly displaced (refugees, asylum seekers, and IDPs), those who had found a long-term solution (returnees), together with stateless persons, and others [7]. The year-on-year trend is constantly rising, a fact that is directly reflected in the area covered by IDP/refugee camps.

Accurate estimates of refugee populations are essential for the planning and management of efficient relief operations and the proper allocation of resources. The number of dwellings in a camp can be used to estimate the refugee population [8]–[10] or monitor changes [11], [12]. Although these tasks can be performed manually, based on the visual interpretation of highly accurate remote sensing data, (semi)automated methods, including multisensor machine learning [13], object-based classification [14], [15], or approaches based on mathematical methods [16], [17], could improve the efficiency of processing workflows. In this context, Ouzounis *et al.* [18], [19] presented image differentials that have been found to be useful in classification problems, including the visualization of human settlements. Differential area profiles, such as derivatives of morphological profiles [20], can be computed directly from granulometries obtained by the successive implementation of morphological attribute filters [21]–[23]. A new, compact representation of morphological profiles is presented in [24]. In the latter study, the authors develop a model that aims to reduce the dimensionality of the decomposition, in a statistical-model-free approach.

A different approach is presented in [25] and [26]. Here, the authors present a fast, interactive method for collecting representative descriptors of objects of interest based on a Max-tree hierarchical image representation [27] that trains the classifier. Training samples are contained within manually selected image regions. In [25], IDP camp structures are extracted based on area, scale, contrast, and compactness metrics. In [26] additionally the k-d tree [28], a hierarchical clustering algorithm is employed to manage the feature space organizations, allowing the classification of a massive image dataset in near real-time.

The abovementioned systematic development and optimization of algorithms based on mathematical morphology has confirmed their usefulness in describing structures, including the footprint of a single dwelling in a camp.

Manuscript received July 1, 2019; revised September 19, 2019 and October 22, 2019; accepted October 28, 2019. Date of publication November 27, 2019; date of current version December 30, 2019. This work was supported by the National Science Centre, Poland, under Grant 2016/23/B/ST10/01151. *(Corresponding author: Małgorzata Jenerowicz.)*

M. Jenerowicz, A. Wawrzaszek, M. Krupiński, and S. Aleksandrowicz are with the Earth Observation Department, Space Research Centre, Polish Academy of Sciences, Warsaw 00-716, Poland (e-mail: mjenerowicz@cbk.waw.pl; sanna@cbk.waw.pl; mkrupinski@cbk.waw.pl; saleksandrowicz@cbk.waw.pl).

W. Drzewiecki is with the Department of Geoinformation, Photogrammetry and Remote Sensing of Environment, AGH University of Science and Technology, Krakow 30-059, Poland (e-mail: drzewiec@agh.edu.pl).

Digital Object Identifier 10.1109/JSTARS.2019.2950970

The analysis presented here explores and tests the effectiveness and capabilities of different approaches to the extraction of data regarding the area covered by a camp, without focusing on single dwelling.

Information about the area covered by a camp may support monitoring of their uncontrolled growth and terrain complexity mapping. Additionally, the response to crises or the regular monitoring of large areas over long periods requires methods that are less time-consuming and labor intensive. Given these requirements, the proposed method is evaluated with the respect to potential automation and independence from reference data.

The proposed approach is based on a multifractal description, which has been applied in remote sensing data analysis. Some of the earliest applications were radar data analysis [29], [30] and the description of VHR optical data [31]–[34]. In an earlier analysis, we found that multifractal parameters were a useful tool for the processing and analysis of large datasets consisting of selected fragments of VHR panchromatic images collected by the EROS-A [31], WorldView-2 [32]–[35], GeoEye-1, and Pléiades-1A [36] satellites. The results of the aforementioned research confirmed the multifractal nature of the analyzed data.

The multifractality parameter that we propose to use to describe that the inhomogeneity of the considered data is at its maximum for developed areas (see, for example, [32] and [34]) and for camp areas characterized by high spatial complexity [36]. To the best of our knowledge, this is the first time multifractal parameters have been determined for large sections of VHR data to investigate the area covered by residential camps.

We extend our previous work by applying the multifractal description to the identification of existing IDP/refugee camps. In particular, the main aim of this analysis is to distinguish residential areas from other land use/land cover types present at two test sites: Dorti and Ardamata (the Al Geneina IDP camp complex in Sudan) and the Ifo and Ifo 2 refugee camp complex in Kenya.

This article is organized as follows. The study area, input, and reference data are described in Section II. In Section III, we briefly discuss our methodology. Section IV presents the results of the multifractal analysis of IDP/refugee camps, showing, in particular, the multifractal map for the considered data. Section V concludes this article.

II. Study Site and Data

A. Study Site

Two test sites were selected as study areas. The first is in Sudan: the Dorti and Ardamata IDP camps; and the second is in Kenya: the two Ifo refugee camps.

Both Dorti and Ardamata camps are located north-east of Al Geneina, West Darfur State, Sudan [37], [38]. They are almost connected to each other and are homogeneous with nearby residential areas that have a similar internal structure, i.e., dwellings bounded by fences in almost square compounds that are separated by roads. Typical dwellings are traditional round huts or tents [39]. These similarities make them recognized as a group of the Al Geneina camps. Consequently, for the sake of simplification, they are hereinafter referred to as the Al Geneina camps.

The Ifo refugee camp complex is located close to Dadaab in Garissa County, Kenya [40]. It consists of two spatially separated parts: the southern part (Ifo) and the northern part (Ifo 2). Ifo 2 was an extension that was officially approved by Kenyan authorities on July 14, 2011 [41]. Hereinafter, they are referred to as the Ifo camps. Their internal structure is similar to that of the Al Geneina camps, but differs with regard to the typical type of dwelling. Here, most dwellings are tented shelters or flat-roofed buildings covered by plastic sheets or tents. Dwelling size, their orientation, materials, and density are homogenous over both of the Ifo camps [41].

In both, Al Geneina and Ifo camps, the minimal dwelling size is four square meters [17], which corresponds to 16 square pixels at the spatial resolution of the data used (see Table I). This information is used to determine the minimal size of the calculation window (see Section IV).

TABLE I
Main Characteristics of the Dataset and the Number of Calculation Windows

	GeoEye-1	Pléiades-1A
Location	Al Geneina	Ifo
Time of acquisition	May 2009	December 2013
Spatial res. [m]	0.5	0.5
Spectral band	PAN	PAN
Intensity range	210−2047	421−4196
Area [pixels]	10240 × 10496	14080 × 14848
Calculation windows	1640	3190

B. Satellite Data

The analysis was run for the two IDP/refugee camps. Monitoring the complex terrain in these areas requires the use of VHR satellite imagery. Here, a set of two VHR PAN satellite image samples were tested [see Fig. 1(a) and (b)]. Table I presents the main characteristics of the dataset and the number of per-image calculation windows (as an indicator of the computational effort).

C. Reference Data

Reference data were derived manually from the visual interpretation of satellite images, supported by maps and other information [41]–[44]. Reference data are limited to a binary mask of the camp area. Fig. 4(a) and (b) presents the mask with original images in the background.

III. Methods

In the analysis presented here, the image is treated as a multifractal that is a nontrivial combination of a number of fractals. Hence, the description of the inner structure, which is the result of intertwined fractals, demands the consideration of the whole spectrum of generalized dimensions D_q [45], [46]. This is in contrast to the fractal case, where only one fractal dimension is studied. In general, the multifractal approach tries to extract information directly from singularities observed in the analyzed data. For homogeneous structures, multifractality tends to zero. This feature distinguishes multifractals from other methods, such as mathematical morphology, which aim to obtain smoother versions of the image by removing irregularities [47].

The multifractal description of the image can be obtained by several methods (e.g., [48]). In this article, we apply the box-counting-based moment (BCBM) method [34] to estimate the function D_q as this method has been successfully tested in many applications for remote sensing data analysis [35],

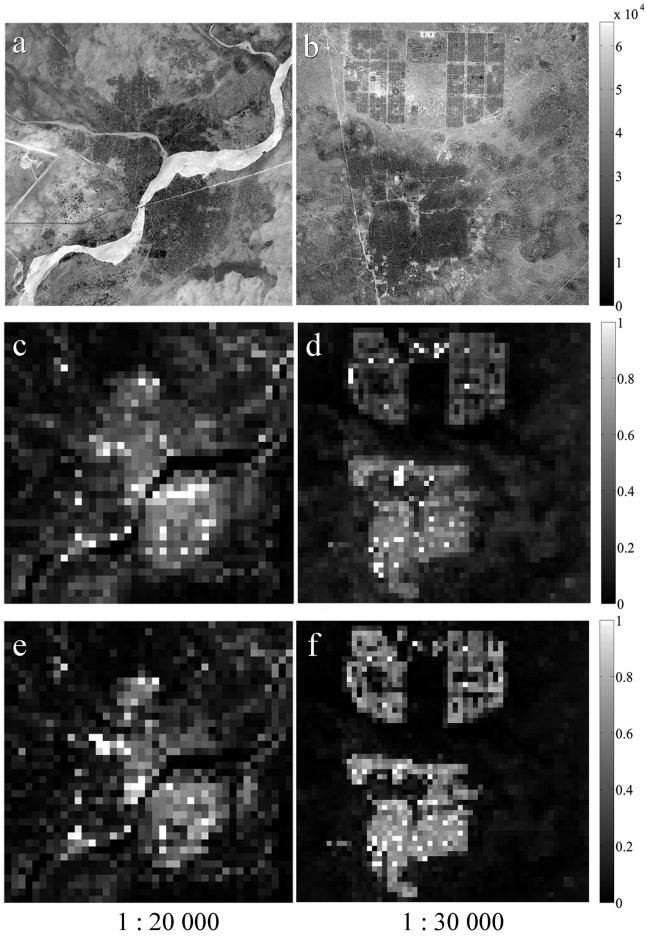

Fig. 1. Original images of the Al Geneina (a) and Ifo (b) camps presented in grayscale with image stretching applied. Multifractal maps are presented in grayscale for Al Geneina (left panel) and Ifo camps (right panel) based on a 256 × 256 pixel window with image stretching applied: (c) and (d) SUM and (e) and (f) MAX measure.

[49]. A detailed explanation of the method can be found in other publications [33]–[35]; a schematic diagram is presented in [34].

In the first step of the BCBM method, an $m \times m$ image is divided into $N(\delta) = (m/\delta)^2$ square boxes of size $\delta \times \delta$, starting with a single pixel $\delta = 1$, and ending with an image box of size $\delta = m$, (see [34, Fig. 1]). Next, for a given box, the normalized measure is calculated according to the following formula:

$$\mu_i(\delta) = \frac{p_i(\delta)}{\sum_{i=1}^{N(\delta)} p_i(\delta)} \tag{1}$$

where $i = 1, \ldots, N(\delta)$ labels individual boxes sized δ, and $p_i(\delta)$ denotes the sum of pixel values in the ith box (SUM) or the maximum gray level in a given box (MAX). Here, $p_i(\delta)$ can be interpreted as the weight of the *i*th box, whereas the denominator in (1) is the total weight of the image. Therefore, $\mu_i(\delta)$ denotes the relative weight of the *i*th box or the probability assigned to the *i*th box [35]. It is worth noting that the SUM measure makes it possible to investigate the self-similarity of the image, whereas the MAX measure makes it possible to analyze the distribution of bright objects, based on the highest pixel values [35]. In the next step, the partition function $\chi(q,\ \delta)$ for various box sizes δ and real moments q is defined as follows:

$$\chi(q,\ \delta) = \sum_{i=1}^{N(\delta)} (\mu_i(\delta))^q. \tag{2}$$

Analyzing the partition function (2), we can control and describe how moments q of measure (1) scale with δ [49]. In particular, for a multifractal structure, the partition function scales with the box size $\delta \rightarrow 0$ as follows:

$$\chi(q,\ \delta) \propto \delta^{D_q(q-1)} \tag{3}$$

where D_q denotes the generalized dimension. From (2) and (3), we obtain the spectrum of generalized dimensions D_q defined by [46]

$$D_q = \frac{1}{1-q} \lim_{\delta \rightarrow 0} \frac{\log \sum_{i=1}^{N(\delta)} (\mu_i(\delta))^q}{-\log \delta}. \tag{4}$$

It is worth noting that the case when $q = 0$ corresponds to the capacity dimension

$$D_0 = \lim_{\delta \rightarrow 0} \frac{\log N(\delta)}{-\log \delta} \tag{5}$$

which should be interpreted as the fractal dimension of the support of the measure. Moreover, for $q \rightarrow +\infty$, the largest value $\mu_{\max}$ dominates the sum in (4) and we have $D_{+\infty} = \lim_{\delta \rightarrow 0} \frac{\log \mu_{\max}}{\log \delta}$ [46], [50]. In the case when $q \rightarrow -\infty$, the smallest value $\mu_{\min}$ dominates the sum and $D_{-\infty} = \lim_{\delta \rightarrow 0} \frac{\log \mu_{\min}}{\log \delta}$.

Variability of the multifractal function D_q is given as the difference between the maximum $(D_{-\infty})$ and minimum $(D_{+\infty})$ dimensions as follows:

$$\Delta \equiv D_{-\infty} - D_{+\infty}. \tag{6}$$

This quantifies the degree of multifractality and quantitatively describes the inhomogeneity of analyzed data [51]. It is worth noting that due to the limited dataset, we can only determine values of D_q for narrow range of moments q. In this study, we analyzed $-5 \leq q \leq 5$, and Δ is calculated as the difference between D_{-5} and D_{+5}. However, errors in the calculation of generalized dimensions for positive q are smaller than for $q < 0$. Therefore, in the final step, Δ_p was used as the difference between D_0 and D_{+5} as uncertainties are lower compared with Δ.

Moreover, results for positive moments q allow to take into account the high concentration of measure (regions of the image with high-intensity values); these areas dwarf smaller ones, a feature that seems to be useful in the description of urban areas [35].

IV. Results

The multifractal analysis used the methodology described in Section III. Selected camp areas were divided into non overlapping 256 × 256-pixel windows. This size was a compromise between the minimum size of camp dwellings found on image samples and the computational effort required to process VHR data (see Section II-B). It was run independently for each window and a degree of multifractality Δ_p was assigned.

Fig. 1(a) and (b) presents original images of the Al Geneina and Ifo camps, respectively, and maps of the degree of multifractality for Al Geneina (left panel) and Ifo (right panel) camps calculated using the SUM measure [see Fig. 1(c) and (d)] and the MAX measure [see Fig. 1(e) and (f)]. All images are presented in grayscale with image stretching applied. Original pixel value

TABLE II
DEGREE OF MULTIFRACTALITY Δ_p VALUES CALCULATED FOR THE WHOLE IMAGE SAMPLE USING A 256 × 256 WINDOW SIZE (R_{org}); USING MANUAL IMAGE INTERPRETATION (R_{man}), THE ROC ANALYSIS (R_{ROC}), AND USING OTSU'S METHOD (R_{Otsu})

	Degree of multifractality Δ_p			
	Al Geneina		Ifo	
	SUM	MAX	SUM	MAX
R_{org}	0.000–0.107	0.000–0.179	0.000–0.155	0.000–0.187
R_{man}	0.002–0.107	0.000–0.179	0.001–0.155	0.000–0.187
R_{ROC}	0.010–0.107	0.008–0.179	0.010–0.155	0.008–0.187
R_{Otsu}	0.016–0.107	0.020–0.179	0.019–0.155	0.030–0.187

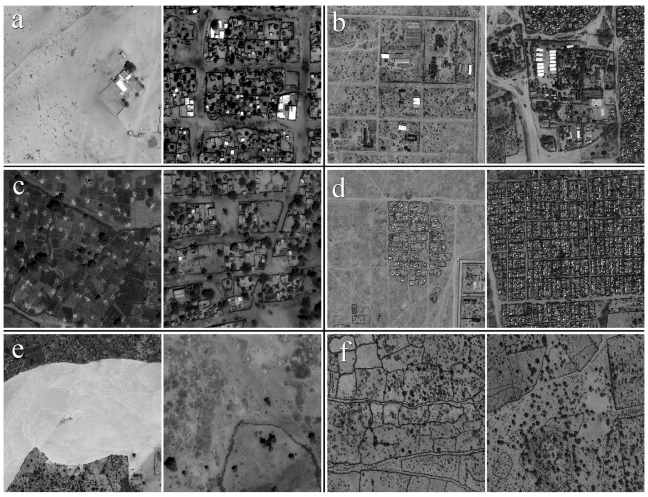

Fig. 2. Selected land use/land cover types found on sample images of Al Geneina [left panel: (a), (c), and (e)] and Ifo [right panel: (b), (d), and (f)] camps, determined using the multifractal method: high-contrast areas indicate functional buildings (a) and (b), homogeneous areas are dwellings or cultivated areas (c) and (d) or sparse vegetation, rivers and bare soil (e) and (f).

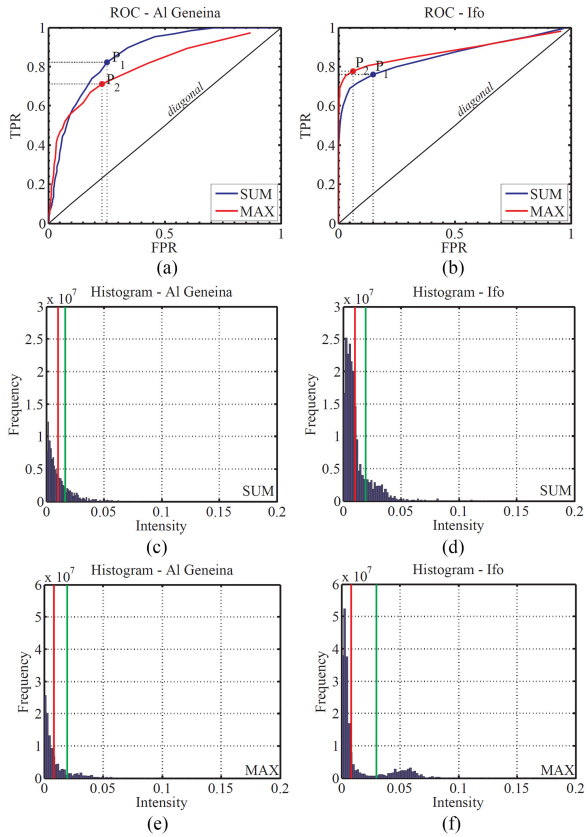

Fig. 3. Results of the analysis of Al Geneina (left panel) and Ifo (right panel) camps areas: ROC curve (a) and (b). Multifractal histograms Δ_p determined using SUM (c) and (d) and MAX measures (e) and (f). Thresholds are calculated using the ROC analysis (red line) and Otsu's method (green line).

ranges are presented in Table I, for input data, and Table II, for output data. The key point to note when comparing the original data and processed data is that for both measures (i.e., SUM and MAX), parameter Δ_p is highest in areas where functional buildings or other high-contrast structures are present. These objects can be either clearly separated from the typical camp dwelling area or adjacent to it [see Fig. 2(a) and (b)]. The average range of Δ_p values refers to homogeneous dwellings or cultivated areas [see Fig. 2(c) and (d)]. Lowest Δ_p values corresponds to sparse vegetation, reaching minimum for bare soil and rivers [see Fig. 2(e) and (f)].

The threshold for classification into camp and noncamp areas was determined using two independent approaches. The first requires the use of reference data and is based on the receiver operating characteristic (ROC) curve analysis [52]. The ROC graph is a simple technique for the visualization, organization, and selection of the best classification thresholds based on true positive rates (TPR) and false positive rates (FPR) derived from the confusion matrix.

It includes correct and incorrect indications (or nonindications) of the class (true positive—TP, true negative—TN, false positive—FP, and false negative—FN). Since the TPR only provides information about the producer's accuracy, user's accuracy was calculated as the positive predictive value (PPV). Overall accuracy (OA) and the Kappa coefficient were also computed.

The threshold is set by calculating optimal classification points (P_1 and P_2) as the minimal distance from the point (0, 1).

The results of the ROC curve analysis for Al Geneina and Ifo camps are presented in Fig. 3. More precisely, Fig. 3(a) and (b) shows optimal classification points for the SUM measure P_1 (blue dot) and the MAX measure P_2 (red dot).

In addition, Fig. 3 presents histograms of multifractality determined using the SUM (c and d) and MAX (e and f) measures. Threshold calculated using the ROC analysis is indicated by red line.

The second approach to the automatic and unsupervised determination of the classification threshold is based on the method proposed by Otsu [53]. In contrast to the ROC analysis, this approach is independent of reference data.

The threshold is set by calculating the separability value on the image histogram. This threshold is indicated in Fig. 3(c)–(f) by green line.

Table II summarizes the range of the degree of multifractality values (Δ_p) for our results, before thresholding, and for the whole image (R_{org}), the manually derived camp area mask (R_{man}), after thresholding performed with the ROC-based approach (R_{ROC}), and Otsu's method (R_{Otsu}). The ranges of Δ_p values presented in Table II are similar, and this seems to be related to the fact that open spaces are also found within camps. Manual mapping does not exclude these open spaces. It should be noted that the minimal Δ_p value is lower in the case of R_{man} than for R_{ROC} and R_{Otsu} cases.

TABLE III
STATISTICAL MEASURES CALCULATED USING AN ROC ANALYSIS BASED ON OPTIMAL CLASSIFICATION POINTS GIVEN IN FIG. 2(A) AND (B) AS P_1 AND P_2

	Degree of multifractality Δ_p			
	Al Geneina		Ifo	
	SUM	MAX	SUM	MAX
TP	18227468	15728293	45200601	46313103
TN	63726464	65618201	128767478	141152172
FP	21618420	19726683	25840423	13455729
FN	3906688	6405863	9251338	8138836
FPR	0.2533	0.2311	0.1671	0.0870
TPR	0.8235	0.7106	0.8301	0.8505
PPV	0.4574	0.4436	0.6363	0.7749
OA	0.7625	0.7569	0.8321	0.8967
Kappa	0.4399	0.3921	0.6034	0.7401

Note: Values for TP, TN, FP, and FN are given in pixels.

TABLE IV
STATISTICAL MEASURES CALCULATED USING THE OTSU APPROACH

	Degree of multifractality Δ_p			
	Al Geneina		Ifo	
	SUM	MAX	SUM	MAX
TP	13211421	10717752	32758031	37691371
TN	76011921	80530604	151845420	152715528
FP	9332963	4814280	2762481	1892373
FN	8922735	11416404	21693908	16760568
FPR	0.1094	0.0564	0.0179	0.0122
TPR	0.5969	0.4842	0.6016	0.6922
PPV	0.5860	0.6900	0.9222	0.9522
OA	0.8301	0.8490	0.8830	0.9108
Kappa	0.4842	0.4809	0.6578	0.7459

Note: Values for TP, TN, FP, and FN are given in pixels.

The results of the assessment of the accuracy of the derived camp masks with respect to reference data (see Section II-C) are presented in Tables III and IV. The results of the multifractal analysis of the Al Geneina and Ifo camp areas are presented in Fig. 4. More precisely, Fig. 4(a) and (b) shows results that are derived manually, whereas Fig. 4(c) and (d) and Fig. 4(e) and (f) use (semi)automatic process based on the degree of multifractality Δ_p determined using SUM and MAX measures, respectively.

The visual interpretation of the obtained results (see Fig. 4) and the derived numerical values (Tables II–IV) lead to the following observations. Both SUM and MAX measures, which are used in the degree of multifractality calculation, reveal the compact structure of the Al Geneina camps and the adjoining residential area [see Fig. 4(c), (e), (g), and (i)] and highlight the Ifo camps area [see Fig. 4(d), (f), (h). and (j)].

The manually derived camp area mask (i.e., reference data), considers the camp area as one unit without separating it into a built-up area and an open space. Unlike the automatically-derived results, it excludes areas characterized by dispersed dwellings. This is clearly visible in Fig. 4(d), (f), (h), and (j), which shows the northern part of the Ifo camps where open spaces are present. In these areas, the degree of multifractality is lower than the minimal values R_{ROC} and R_{Otsu} listed in Table II.

Although Otsu's method gives fewer FP, the final mask of the Al Geneina camps does not include northern and eastern areas that are sparsely covered by dwellings [see Fig. 4(g) and (i)]. This increases the incidence of FN, which are more frequent using Otsu's method compared with the ROC analysis (Tables III and IV). The high FPR, especially for the ROC analysis (see Table III), is due to high multifractality values used in calculation

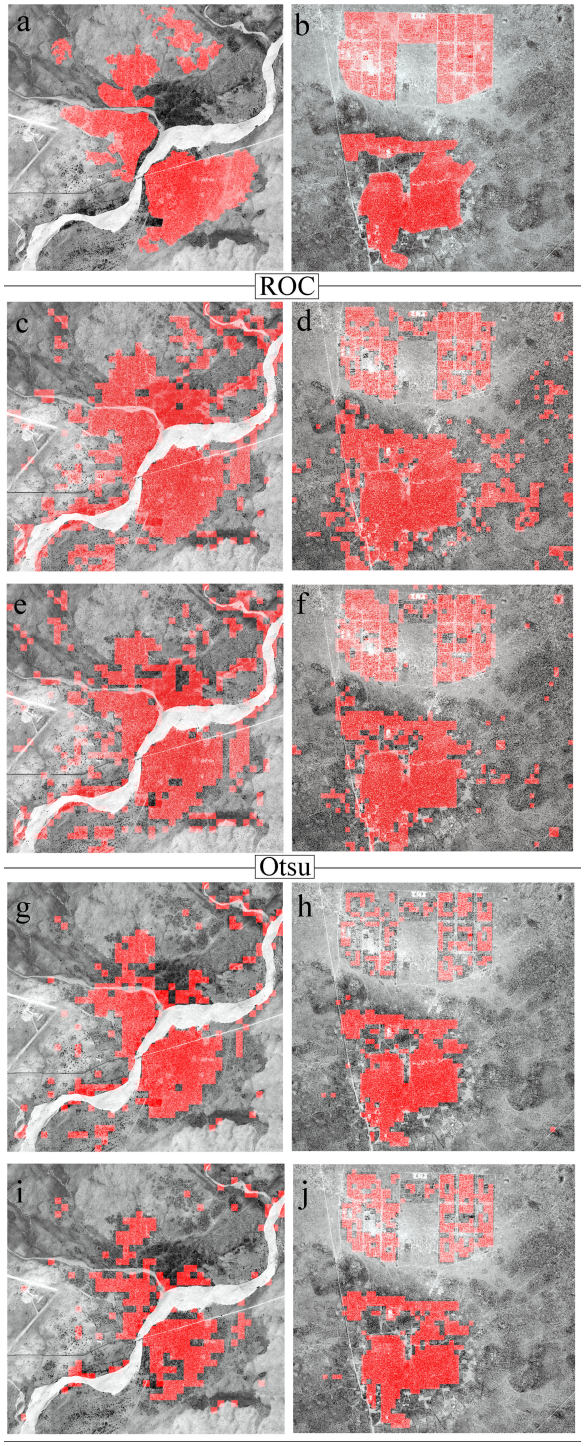

Fig. 4. Al Geneina (left panel) and Ifo (right panel) camps masks derived: manually by visual interpretation (a) and (b), via the multifractality method where Δ_p is calculated using SUM (c), (d), (g), and (h) and MAX measures (e), (f), (i), and (j). Classification thresholds are determined based on a ROC analysis and Otsu's method.

windows. These values represent the most homogenous areas with few irregularities (e.g., a high-contrast road, bare rock, a river bank, or farming infrastructure). This singularity can strongly influence the calculation by increasing the final degree of multifractality.

An analysis of the accuracy of the detection results leads to the following remarks. For the ROC analysis, the SUM measure works better when applied to the Al Geneina camps than the Ifo camps—where the MAX measure is more accurate. For the analysis performed using Otsu's method, the MAX measure dominates for the Ifo camps, but in the case of the Al Geneina camps, the OA and the Kappa coefficient indicate comparable results for SUM and MAX measures. These differences can only be detected by comparing user's and producer's accuracies.

In general, results for the Ifo camps are significantly better than for the Al Geneina camps, both in terms of sensitivity and precision. Moreover, a comparison of Otsu's method and the ROC analysis shows that producer's accuracy decreases and user's accuracy increases: TPR 85% and PPV 77% were obtained in the ROC analysis (see Table III) compared with TPR 69% and PPV 95% based on Otsu's method (see Table IV). OA and the Kappa coefficient are higher for results obtained automatically using Otsu's method. They ranges from 83% OA (48% Kappa) for Al Geneina camps to 91% OA (75% Kappa) for Ifo camps. Differences in accuracy parameters for the two camps are most probably due to differences in their spatial complexity (see Section II-A).

V. Conclusion

In the frame of this article, we performed multifractal analysis aimed to identify the extent of two IDP/refugee camps in Sudan and Kenya. Our results show that the degree of multifractality calculated for the selected images increases for compact areas with high-contrast structures (e.g., functional buildings and dwellings). This observation seems to confirm the conclusions obtained in [34], where an analysis of four types of land cover (water, agriculture, forest, and urban) found the highest multifractality for urban areas. However, it should be noted that Wawrzaszek *et al.* [34] applied a much bigger calculation window (1024×1024 pixels) and sample images were preselected. Our results are also consistent with the findings reported in [36], although this study only examined a small sample of the camp area in order to test the applicability of multifractal features as descriptors of complex terrain.

The extraction of the IDP/refugee camps extent by using only one feature, i.e., the degree of multifractality, proved to be an efficient way for initial image classification. It should be noted, however, that spatial accuracy depends on the spatial complexity of the surrounding area. Although all of the obtained results are characterized by high OA, it should be noted that in the case of binary classification of unbalanced classes, the PPV and Kappa coefficient are considered as more relevant measures for accuracy determination. Results obtained for Ifo camps are significantly better than for the Al Geneina camps, both in terms of sensitivity and precision. For Al Geneina camps, the presence of dense, heterogeneous shrubby areas, roads, and riverbanks adjacent to vegetation increased the FPR. Regardless of camp and multifractal measure, PPV and Kappa coefficient are higher for Otsu's method where the FPR decreased, although this comes at the cost of an increase in FN. Therefore, other thresholding methods should also be explored.

Our work is a preliminary test of the usefulness of multifractal analysis in studies of camp areas. Further research would help to improve our results. Postprocessing could reduce both FP and FN. Simple (e.g., majority voting) or more sophisticated (e.g., morphological operators) approaches could be used to fill gaps within camps or to filter out small, isolated areas classified as camp. Additionally, we expect that camps characterized by low contrast levels will decrease the effectiveness of the proposed method. However, our earlier work [34] suggests that preprocessing with various filters can help to maintain a sufficient level of class separability. Nevertheless, it is clear that the effectiveness of the presented approach in analyzing low-contrast areas requires further study.

Our approach has been tested on panchromatic bands. The use of additional spectral information derived from multispectral images may significantly increase accuracy. FP could be reduced by supplementing the analysis with a vegetation index, such as the normalized difference vegetation index; this option should be investigated in future work.

Furthermore, our study shows that approaches, such as Otsu's method, can be used in the automatic determination of the spatial complexity threshold, based on the degree of multifractality.

Consequently, the proposed method is characterized by a high degree of automation compared with manual mapping, which generally involves an expert in the domain and additional maps and information. Increasing automation can help to provide results more quickly, with more frequent updates. This is an important asset if the camp is growing rapidly, especially for tasks that require repeated, rapid, and rough estimates of the camp's extent.

Our work is ongoing, and future studies will focus on testing the method on a larger dataset, the inclusion of multispectral bands, analyzing other areas of interest, and examining the added value of other multifractal measures (see, e.g., [35]) including the local approach [54], [55]. We will continue to identify ways to improve classification accuracy and will focus on the development of an unsupervised classification approach that will be based on the combination of several multifractal measures, rather than a single feature. This may also improve the distinction between camp areas and nearby settlements.

We would also like to test the potential of an extended set of multifractal parameters to provide a more detailed description of the area covered by a camp. The correspondence between the degree of multifractality and land cover type revealed by previous studies [34], [35] was also observed for camp areas and their surroundings. It remains to be seen if this feature could be used to differentiate different camp zones (e.g., areas with functional buildings and dwellings, or areas covered by various dwelling densities).

Finally, in the next phase of our work, we plan to perform a more systematic and detailed analysis of differences between mathematical morphology and multifractal-based approaches and indicate possible areas where they interact (see, e.g., [56]).

Acknowledgment

The dataset was made available under the cooperation agreement between the Space Research Centre of the Polish Academy of Science and the European Commission's Joint Research Centre.

References

[1] L. Xi, C. Fengrui, and C. Xiaoling, "Satellite-observed nighttime light variation as evidence for global armed conflicts," *IEEE J. Sel. Topics Appl. Earth Observ. Remote Sens.*, vol. 6, no. 5, pp. 2302–2315, Oct. 2013.

[2] F. D. W. Witmer, "Remote sensing of violent conflict: Eyes from above," *Int. J. Remote Sens.*, vol. 36, p. 2326, 2015.

[3] O. Kranz, A. Sachs. and S. Lang, "Assessment of environmental changes induced by internally displaced person (IDP) camps in the Darfur region, Sudan, based on multitemporal MODIS data," *Int. J. Remote Sens.*, vol. 36, no. 1, pp. 190–210, 2015.

[4] D. Contreras, T. Blaschke, D. Tiede, and M. Jilge, "Monitoring recovery after earthquakes through the integration of remote sensing, GIS, and ground observations: The case of L'Aquila (Italy)," *Cartogr. Geographic Inf. Sci.*, vol. 43, no. 2, pp. 115–133, 2016.

[5] A. Marx and S. Goward, "Remote sensing in human rights and international humanitarian law monitoring: Concepts and methods," *Geographical Rev.*, vol. 103, no. 1, pp. 100–111, 2013.

[6] F. D. W. Witmer, "Remote sensing of violent conflict: Eyes from above," *Int. J. Remote Sens.*, vol. 36, no. 9, pp. 2326–2352, 2015.

[7] United Nations High Commissioner of Refugees (UNHCR). Global Trends, Forced Displacement in 2018, 2018. [Online]. Available: https://www.unhcr.org/globaltrends2018/

[8] S. Giada, T. DeGroeve, D. Ehrlich, and P. Soille, "Information extraction from very high resolution satellite imagery over Lukole refugee camp, Tanzania," *Int. J. Remote Sens.*, vol. 24, pp. 4251–4266, 2003.

[9] T. Kemper, M. Jenerowicz, M. Pesaresi, and P. Soille, "Enumeration of dwellings in Darfur camps from GeoEye-1 satellite image using mathematical morphology," *IEEE J. Sel. Topics Appl. Earth Observ. Remote Sens.*, vol. 4, no. 1, pp. 8–15, Mar. 2011.

[10] M. Jenerowicz and T. Kemper, "An automated procedure for detection of IDP's dwellings using VHR satellite imagery," *Proc. SPIE*, vol. 8180, 2011, Art. no. 818004.

[11] T. Kemper, M. Jenerowicz, L. Gueguen, D. Poli, and P. Soille, "Monitoring changes in the Menik Farm IDP camps in Sri Lanka using multi-temporal very high-resolution satellite data," *Int. J. Digital Earth*, vol. 4, no. sup1, pp. 91–106, 2011.

[12] C. Knoth and E. Pebesma, "Detecting dwelling destruction in Darfur through object-based change analysis of very high-resolution imagery," *Int. J. Remote Sens.*, vol. 38, no. 1, pp. 273–295, 2017.

[13] P. Aravena Pelizari, K. Sprohnle, C. Geib, E. Schoepfer, S. Plank, and H. Taubenbock, "Multisensor feature fusion for very high spatial resolution built-up area extraction in temporary settlements," *Remote Sens. Environ.*, vol. 209, pp. 793–807, 2018.

[14] S. Lang, D. Tiede, D. Hölbling, P. Füreder, and P. Zeil, "Earth observation (EO)-based ex post assessment of internally displaced person (IDP) camp evolution and population dynamics in Zam Zam, Darfur," *Int. J. Remote Sens.*, vol. 31, no. 21, pp. 5709–5731, 2010.

[15] K. Spröhnle, E. M. Fuchs, and P. Aravena Pelizari, "Object-based analysis and fusion of optical and SAR satellite data for dwelling detection in refugee camps," *IEEE J. Sel. Topics Appl. Earth Observ. Remote Sens.*, vol. 10, no. 5, pp. 1780–1791, May 2017.

[16] S. Wang, E. So, and P. Smith, "Detecting tents to estimate displaced populations for post-disaster relief using high resolution satellite imagery," *Int. J. Appl. Earth Observ. Geoinf.*, vol. 36, pp. 87–93, 2015.

[17] M. Jenerowicz and T. Kemper, "An improved automated procedure for informal and temporary dwellings detection and enumeration, using mathematical morphology operators on VHR satellite data," *Proc. SPIE*, vol. 10008, 2016, Art. no. 100080O.

[18] G. K. Ouzounis and P. Soille, "Pattern spectra from partition pyramids and hierarchies," in *Proceedings on the 10th International Symposium on Mathematical Morphology and Its Applications to Image and Signal Processing* (Lecture Notes in Computer Science), P. Soille, M. Pesaresi, and G. K. Ouzounis, Eds. Berlin, Germany: Springer, 2011, pp. 108–119.

[19] G. K. Ouzounis, M. Pesaresi, and P. Soille, "Differential area profiles: Decomposition properties and efficient computation," *IEEE Trans. Pattern Anal. Mach. Intell.*, vol. 34, no. 8, pp. 1533–1548, Aug. 2012.

[20] M. Pesaresi and J. A. Benediktsson, "A new approach for the morphological segmentation of high-resolution satellite imagery," *IEEE Trans. Geosci. Remote Sens.*, vol. 39, no. 2, pp. 309–320, Feb. 2001.

[21] E. J. Breen and R. Jones, "Attribute openings, thinnings and granulometries," *Comp. Vis. Image Understand.*, vol. 64, no. 3, pp. 377–389, 1996.

[22] L. Vincent, "Granulometries and opening trees," *Fundamenta Informaticae*, vol. 41, no. 1–2, pp. 57–90, 2000.

[23] E. R. Urbach, J. B. T. M. Roerdink, and M. H. F. Wilkinson, "Connected shape-size pattern spectra for rotation and scale-invariant classification of gray-scale images," *IEEE Trans. Pattern Anal. Mach. Intell.*, vol. 29, no. 2, pp. 272–285, Feb. 2007.

[24] M. Pesaresi, G. K. Ouzounis, and L. Gueguen, "A new compact representation of morphological profiles: report on first massive VHR image processing at the JRC," *Proc. SPIE.*, vol. 8390, 2012, Art. no. 839025.

[25] G. K. Ouzounis and L. Gueguen, "Interactive collection of training samples from the Max-Tree structure," in *Proc. IEEE Int. Conf. Image Process.*, 2011, pp. 1449–1452.

[26] L. Gueguen and G. K. Ouzounis, "Hierarchical data representation structures for interactive image information mining," *Int. J. Image Data Fusion*, vol. 3, no. 3, pp. 221–241, 2012.

[27] P. Salembier, A. Oliveras, and L. Garrido, "Anti-extensive connected operators for image and sequence processing," *IEEE Trans. Image Process.*, vol. 7, no. 4, pp. 555–570, Apr. 1998.

[28] J. Bentley, "Multidimensional binary search trees used for associative searching," *Commun. ACM*, vol. 18, no. 9, pp. 509–517, 1795.

[29] T. Falco, F. Francis, S. Lovejoy, D. Schertzer, B. Kerman, and M. Drinkwater, "Universal multifractal scaling of synthetic aperture radar images of sea-ice," *IEEE Trans. Geosci. Remote Sens.*, vol. 34, no. 4, pp. 905–914, Jul. 1996.

[30] T. S. Yeo and D. Gan, "A multifractal approach for auto-segmentation of SAR images," in *Proc. IEEE Geosci. Remote Sens. Symp.*, 2001, vol. 5, pp. 2301–2303.

[31] W. Drzewiecki, A. Wawrzaszek, M. Krupiński, S. Aleksandrowicz, and K. Bernat, "Comparison of selected textural features as global content-based descriptors of VHR satellite image—the EROS-A study," in *Proc. Federated Conf. Comput. Sci. Inf. Syst.*, 2013, pp. 43–49.

[32] W. Drzewiecki, A. Wawrzaszek, S. Aleksandrowicz, M. Krupiński, and K. Bernat, "Comparison of selected textural features as global content-based descriptors of VHR satellite image," in *Proc. IEEE Int. Geosci. Remote Sens. Symp.*, 2013, pp. 4364–4366.

[33] A. Wawrzaszek, S. Aleksandrowicz, M. Krupiński, and W. Drzewiecki, "Fractal and multifractal characteristics of very high resolution satellite images," in *Proc. IEEE Int. Geosci. Remote Sens. Symp.*, 2013, pp. 1501–1504.

[34] A. Wawrzaszek, S. Aleksandrowicz, M. Krupiński, and W. Drzewiecki, "Influence of image filtering on land cover classification when using fractal and multifractal features," *Photogrammetrie -Fernerkundung - Geoinf.* vol. 2, pp. 0101–0115, 2014.

[35] W. Drzewiecki, A. Wawrzaszek, M. Krupiński, S. Aleksandrowicz, and K. Bernat, "Applicability of multifractal features as global characteristics of WorldView-2 panchromatic satellite images," *Eur. J. Remote Sens.*, vol. 49, pp. 809–834, 2016.

[36] M. Jenerowicz, A. Wawrzaszek, M. Krupiński, W. Drzewiecki, and S. Aleksandrowicz, "Applicability of multifractal features as descriptors of the complex terrain situation in IDP/Refugee camps," in *Proc. IEEE Int. Geosci. Remote Sens. Symp.*, Yokohama, Japan, pp. 2662–2665, 2019.

[37] United Nations Institute for Training and Research, Operational Satellite Applications Programme (UNOSAT-UNITAR), Respond Humanitarian Global Mapping Services Product ID: 196, Sudan/Darfur - Al Junaynah region and Wadi Kaja flood map, Sep. 3, 2004. [Online]. Available: http://unosat-maps.web.cern.ch/unosat-maps/SD/SERTIT_al-junaynah_50k_high.jpeg

[38] United Nations Institute for Training and Research, Operational Satellite Applications Programme (UNOSAT-UNITAR), Respond Humanitarian Global Mapping Services Product ID: 195, Sudan/Darfur - Al Junaynah city and Wadi Kaja flood map, Aug. 27, 2004. [Online]. Available: http://unosat-maps.web.cern.ch/unosat-maps/SD/SERTIT_al-junaynah_25k_high.jpeg

[39] D. Tiede, S. Lang, D. Hölbling, and P. Füreder, "Transferability of OBIA rulesets for IDP camp analysis in Darfur," *Int. Archives Photogramm., Remote Sens. Spatial Inf. Sci*, vol. XXXVIII-4-C7, 2010. [Online]. Available: https://www.isprs.org/proceedings/XXXVIII/4-C7/pdf/Tiede_137.pdf

[40] United Nations High Commissioner of Refugees (UNHCR), Operational Portal Refugee Situations, Kenya—Ifo Refugee Camp Overview, Jan. 2012. [Online]. Available: https://data2.unhcr.org/en/documents/details/31533

[41] United Nations Institute for Training and Research, Operational Satellite Applications Programme (UNOSAT-UNITAR), Update1: Emergency assessment of Ifo Refugee camp, Garissa, N. Eastern, Kenya, Aug. 2011. [Online]. Available:https://data2.unhcr.org/en/documents/download/30899

[42] Reliefweb, Sudan: Ardamata IDP camp - El Geneina, Western Darfur (as of Jul. 22, 2006), Jul. 22, 2006. [Online]. Available: https://reliefweb.int/map/sudan/sudan-ardamata-idp-camp-el-geneina-western-darfur-22-jul-2006

[43] United Nations High Commissioner of Refugees (UNHCR), Operational portal refugee situations, Feb. 15, 2019. [Online]. Available: https://data2.unhcr.org/en/situations/horn/location/182

[44] United Nations Institute for Training and Research, Operational Satellite Applications Programme (UNOSAT-UNITAR), Respond Humanitarian Global Mapping Services Product ID: 194, Sudan/Darfur - Ardamata IDP camp near Wadi Kaja riverbed, Sep. 3, 2004. [Online]. Available: http://unosat-maps.web.cern.ch/unosat-maps/SD/SERTIT_al-junaynah_10k_high.jpeg

[45] T. C. Halsey, M. H. Jensen, L. P. Kadanoff, I. Procaccia, and B. I. Shraiman, "Fractal measures and their singularities: The characterization of strange sets," *Phys. Rev. A*, vol. 33, no. 2, pp. 1141–1151, 1986.
[46] H. Hentschel and I. Procaccia, "The infinite number of generalized dimensions of fractals and strange attractor," *Physica D*, vol. 8, pp. 435–444, 1983.
[47] P. Goncalves J. L. Vehel, and P. Abry, Ed. *Scaling Fractals and Wavelets* (Digital Signal and Image Processing Series). Hoboken, NJ, USA: Wiley, 2002.
[48] R. Lopes and N. Betrouni, "Fractal and multifractal analysis: A review," *Med. Image Anal.*, vol. 13, pp. 634–649, 2009.
[49] A. Wawrzaszek, M. Echim, W. M. Macek, and R. Bruno, "Evolution of intermittency in the slow and fast solar wind beyond the ecliptic plane," *Astrophys. J. Lett.*, vol. 814, p. L19, 2015.
[50] C. Meneveau and K. R. Sreenivasan, "The multifractal nature of the turbulent energy dissipation," *J. Fluid Mechanics*, vol. 224, pp. 429–484, 1991.
[51] A. Szczepaniak and W. M. Macek, "Asymmetric multifractal model for solar wind intermittent turbulence," *Nonlinear Processes Geophys.*, vol. 15, pp. 615–620, 2008.
[52] T. Fawcett, "An introduction to ROC analysis," *Pattern Recognit. Lett.*, vol. 27, no. 8, pp. 861–874, 2006.
[53] N. Otsu, "A threshold selection method from gray-level histograms," *Automatica*, vol. 11, no. 285–296, pp. 23–27, 1975.
[54] S. Aleksandrowicz, A. Wawrzaszek, W. Drzewiecki, and M. Krupiński, "Change detection using global and local multifractal description," *IEEE Geosci. Remote Sens. Lett.*, vol. 13, no. 8, pp. 1183–1187, Aug. 2016.
[55] M. Jenerowicz, A. Wawrzaszek, M. Krupiński, S. Aleksandrowicz, and W. Drzewiecki, "Comparison of mathematical morphology with the local multifractal description applied to the image samples processing," in *Proc. SPIE, Photonics Applications in Astronomy, Communications, Industry, and High-Energy Physics Experiments*, vol. 11176, 2019, doi: 10.1117/12.2536408, Art. no. 1117638.
[56] Y. Xia, D. D. Feng, and R. Zhao, "Morphology-based multifractal estimation for texture segmentation," *IEEE Trans. Image Process.*, vol. 15, no. 3, pp. 614–623, Mar. 2006.

Małgorzata Jenerowicz received the M.S. degree in geoinformatics from the Military University of Technology, Warsaw, Poland, in 2007, and the Ph.D. degree in geophysics from the Space Research Centre, Polish Academy of Sciences (CBK PAN), Warsaw, Poland, in 2016.

In her Ph.D. thesis, she investigated automatic feature extraction based on mathematical morphology and very high resolution satellite imagery (the Rosetta mission and the Earth Observation campaign). Since 2008, she has been with Earth Observation Department, CBK PAN, where her research is focused on remote sensing data analysis. During 2009–2010, she was a temporary Research Assistant with the European Commission's Joint Research Centre, Ispra, Italy. During 2016–2017, she led a project under the Polish–Norwegian Research Cooperation Programme, which aimed to develop an improved, automated procedure for the detection and enumeration of internally displaced persons/refugee dwellings. She is currently a Postdoctoral Researcher with CBK PAN, where her work is focused on evaluating the usefulness of multifractal parameters versus mathematical morphology in the analysis of remote sensing images. Her research interests include the application of mathematical morphology to feature extraction, the development of an operational tool that can be applied in humanitarian support and crisis management, and astronomical objects landform analysis.

Dr. Jenerowicz was the recipient of a ministerial grant for young scientists (in 2018).

Anna Wawrzaszek (M'04) received the bachelor's degree in computer science in 2004 and the M.S. degree in mathematics, in 2004 both from the University of Podlasie, Siedlce, Poland, and the Ph.D. degree in geophysics from the Space Research Centre, Polish Academy of Sciences (CBK PAN) in 2009.

Since 2009, she has been a Physicist with the CBK PAN, where she has been also an Assistant Professor since 2011. She has been involved in a number of projects related to the analysis of large, multidimensional data collected during various space missions. She was a member of the team working on the launch of the first Polish scientific satellites (the BRITE-PL project), which currently has two satellites in orbit. She has authored more than 30 scientific articles. Her research interests include advanced multifractal parameters and their application to the analysis of turbulence in the solar wind, along with the classification, segmentation, and change detection of multispectral and hyperspectral very high resolution imagery data.

Wojciech Drzewiecki received the M.S. and Ph.D. degrees in environmental engineering from the AGH University of Science and Technology, Krakow, Poland, in 1996 and 2003, respectively.

Since 2004, he has been an Assistant Professor with the Department of Geoinformation, Photogrammetry and Remote Sensing of Environment, AGH University of Science and Technology. From 2009 to 2011, he was a Senior Geoinformation Specialist with the Earth Observation Department, Space Research Centre, Polish Academy of Sciences (CBK PAN). Since 2012, he has been with the CBK PAN as a Researcher. He has authored more than 60 scientific publications. His research interests include the classification of remote sensing images and environmental applications of geospatial technologies.

Michał Krupiński (M'12) received the bachelor's and master's degrees in geodesy and cartography from the Military University of Technology, Warsaw, Poland, in 2010 and 2012, respectively.

Since 2010 he has been a Geomatics Specialist with the Space Research Centre, Polish Academy of Sciences. He is involved in a number of scientific and R&D projects focused on geospatial data analysis. His research interests include novel methods for satellite imagery classification and imaging spectroscopy.

Sebastian Aleksandrowicz received the M.S. degree in geoinformatics from the Military University of Technology, Warsaw, Poland, in 2007, and the Ph.D. degree in engineering and technology from the AGH University of Science and Technology, Krakow, Poland, in 2019.

Since 2009, he has been a Geomatics Specialist with the Earth Observation Department, Space Research Centre, Polish Academy of Sciences. He has more than nine years' experience in Copernicus/GMES and European Space Agency projects. His research interests include object-based classification and change detection methods.